PHYSICAL REVIEW B **71**, 041101(R) (2005)

PtN: A zinc-blende metallic transition-metal compound

B. R. Sahu and Leonard Kleinman
Department of Physics, University of Texas at Austin, Austin, Texas 78712-0264, USA
(Received 11 August 2004; revised manuscript received 28 September 2004; published 10 January 2005)

With fully relativistic full potential augmented plane wave calculations we confirm that the recently synthesized compound PtN is crystallized in the zinc-blende structure and is metallic. We find that the density of states consists of four pieces and discuss how each contributes to the bonding.

DOI: 10.1103/PhysRevB.71.041101 PACS number(s): 71.20.Ps, 81.05.Zx

In a recent paper, Gregoryanz *et al.*[1] synthesized platinum nitride (PtN). The compound is formed at high temperature (exceeding 2000 K) and high pressure (above 45 GPa) and was found to be stable after quenching to room temperature and room pressure. Their synchrotron x-ray diffraction analysis reveals that PtN has a face-centered-cubic structure but was unable to distinguish between the zinc-blende (space-group number 216) and rocksalt (space-group number 225) structures. But their Raman spectrum was similar to that of GaN and InN and therefore they concluded that PtN has the zinc-blende structure. This conclusion is quite surprising since all monotransition metal nitrides, CrN, NbN, VN, and ZrN, with the exception of MnN which has 1.6% tetragonal distortion,[2,3] have the NaCl structure. They[1] obtained a lattice constant of $a=4.8041(2)$ Å at ambient conditions as well as bulk modulus $B=372$ (± 5) GPa which is comparable with the $B=382$ (± 3) GPa of the superhard material[4] cubic BN. They also determined that, unlike VN and NbN, PtN is not superconducting (down to 2 K) but could not tell whether it is a poor metal or a narrow gap semiconductor.

To determine the structural and bonding properties of PtN and to determine whether it is a metal or a semiconductor we have performed fully relativistic full potential linearlized augmented plane-wave (APW) calculations.[5] The generalized gradient approximation[6] (GGA) was used for the exchange and correlation energy density functional. Nonoverlapping muffin-tin (MT) sphere radii of 2.2 and 1.5 bohr were used for the Pt and N atoms, respectively. The valence wave functions inside the MT spheres were expanded into spherical harmonics up to $l=10$ and the potential up to $l=8$. An APW plus local valence orbitals[7,8] basis set was used with the Pt 5*s* and 5*p* semicore states treated as valence states. Convergence of total energy with respect to the plane-wave expansion parameter $R_{MT}K_{\max}$ (where R_{MT} is the smaller of the two MT radii and $K_{\max}$ is the plane-wave cutoff) and the **k**-point sampling was checked. Fifty six **k** points in the irreducible wedge of the fcc Brillouin zone and $R_{MT}K_{\max}=8$ turn out be sufficient for accuracy of the calculated total energy (0.01 mRy/unit cell). The calculated total energy versus unit-cell volume was fitted with the Murnaghan equation of state[9] curve and the calculations were repeated at the curve minimum.

In Table I the lattice constants, bulk moduli, and cohesive energies of PtN are compared in the zinc-blende and rocksalt structures with the experimental values from Ref. 1. The zinc-blende lattice constant and bulk modulus are in perfect agreement with experiment, while the rocksalt bulk modulus agrees poorly and its 6.32% error in lattice constant is about three times larger than one might expect for the correct crystal structure. If corrected for anharmonic thermal and zero-point contributions, the experimental lattice constant would be expected to be smaller than our calculated value, consistent with the usual result that GGA lattice constants exceed the experimental values.[10] The cohesive energy, calculated by subtracting the calculated energy of spin-polarized Pt and N atoms from the crystal energy (per unit cell), also favors the zinc-blende structure, by a small but not insignificant amount. These results indicate that at sufficiently high pressure and temperature the rocksalt structure would be favored, and if the temperature were quenched before the pressure was reduced, the rocksalt structure might be metastable. Furthermore, it would have a bulk modulus close to that of diamond. Figure 1 is a plot of cohesive energy as a function of unit-cell volume for the two structures. The slope of the tangent line reveals that, at a pressure of 24 GPa, a transition from zinc-blende to rocksalt would occur if the temperature were high enough to break the zinc-blende covalent bonds. More importantly, these results confirm beyond any reasonable doubt, that the structure synthesized by Gregoryanz *et al.*[1] is zinc-blende. We note that GGA calculations almost always result in lattice constants that are larger than, and bulk moduli smaller than, those obtained from local-density approximation (LDA) calculations. Therefore, had we performed LDA calculations, our rocksalt lattice constant and bulk modulus would be expected to be in even greater disagreement with experiment.

Figure 2 displays the *s*, *p*, and *d* components of the densities of states (DOS) within the Pt and N MT spheres for the zinc-blende PtN. Because the radii of these spheres are somewhat arbitrary, the relative charge within the two

TABLE I. The experimental (Ref. 1) and calculated lattice constants (in bohr), cohesive energies (in eV per atom), and bulk moduli (in GPa) of PtN in the zinc-blende (ZB) and rocksalt (NaCl) structures.

	a	E_{coh}	B
ZB	9.0786	4.573	371.01
NaCl	8.5385	4.352	431.45
Expt.	9.0784		372 (± 5)

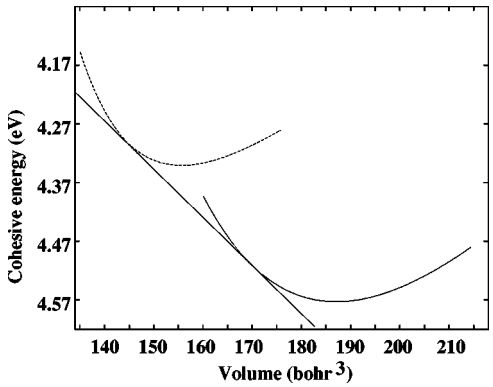

FIG. 1. Cohesive energy per atom (in eV) vs volume per atom (in bohr^3) for PtN in the rocksalt (dashed line) and zinc-blende (solid line) structures, and the tangent line whose slope is 24 GPa.

spheres should not be given too much significance. Figure 3 displays the energy bands around the Fermi energy (E_F). Because of the large Pt 5*d* spin-orbit interaction and the huge asymmetry between N and Pt, many of the bands are nondegenerate, i.e., the Kramers degeneracy exists only between states with **k** and −**k** wave vectors. Note that along the line from *W* to *K* in the Brillouin zone there are 15 nondegenerate bands below E_F plus the two N *s* levels at lower energy. The first thing we note is that PtN is either a metal or a Mott insulator, as it must be, because it contains 15 valence electrons, an odd number, per unit cell. However, all the sharp peaks in the DOS, signifying narrow energy bands, lie well below E_F, and the bands which cross E_F look free-electron-like, especially along the *Q* and Δ lines. Thus we conclude that PtN is a metal. In Fig. 4 we plot the contribution of each

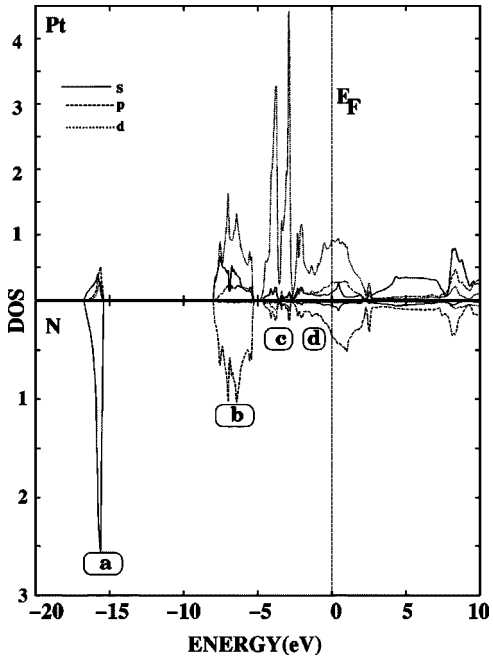

FIG. 2. *s* (solid line), *p* (dashed line), and *d* (dotted line) projected densities of states in the Pt and N spheres of zinc-blende PtN. The *a*, *b*, *c*, and *d* label different regions of the DOS which are discussed in the text.

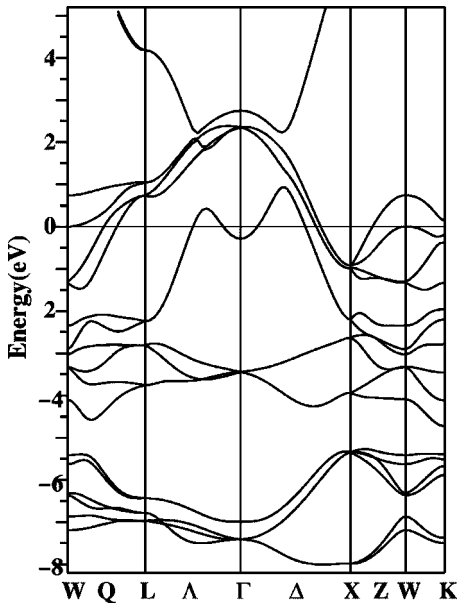

FIG. 3. Energy bands of zinc-blende PtN along high-symmetry directions near the Fermi energy (located at $E=0$). The low-lying N 2*s* bands are not shown.

set of energy bands (labeled *a*, *b*, *c*, and *d* in Fig. 2) to the covalent bonds of zinc-blende PtN.

The *a* electrons are a pair of essentially N 2*s* bands which are degenerate along the Λ and Δ lines but slightly spin-orbit split on the Brillouin zone faces. Although their charge density becomes infinitesimal three quarters of the way to the Pt atom, their contribution to the covalent bond at its minimum is not negligible. The major contribution to the covalent bonds come from the *b* electrons consisting of six strongly hybridizing bands of N 2*p* and Pt 5*d* electrons with smaller Pt 6*s* and 6*p* components. The four Pt 5*d* bands of *c* electrons overlap the continuum of electrons in the *d* region (but do not in the absence of spin-orbit splitting). Nevertheless we do not treat them as part of the continuum because they result in very large peaks in the DOS. The *d*-electron charge lobes of the *c* electrons point much more strongly in the (011) direction than in the (111) so they do not contribute much to the covalent bonding. The *d* region consists of the

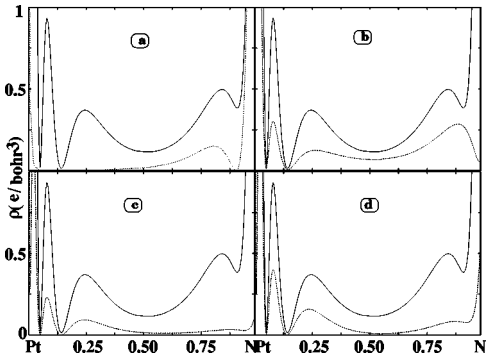

FIG. 4. Comparision of the valence charge density coming from the four energy ranges in the DOS labeled *a*, *b*, *c*, and *d* in Fig. 2 (dashed line) with the total charge density from all four regions (solid line).

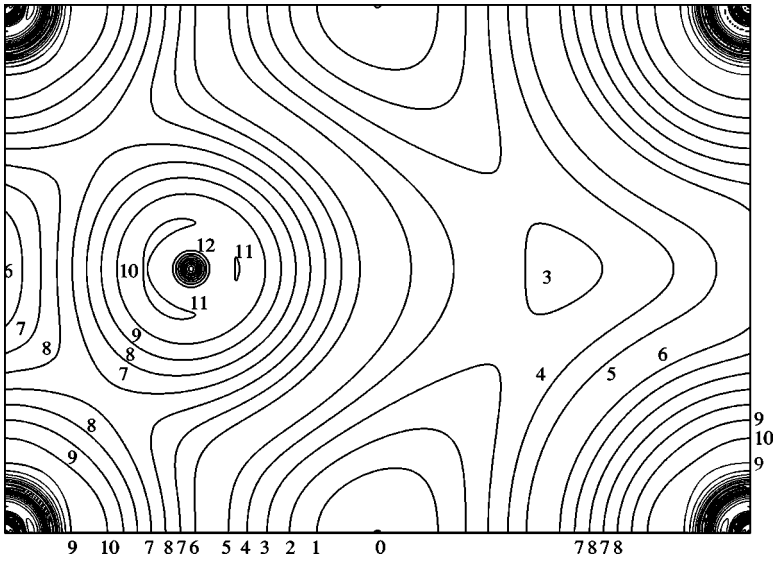

FIG. 5. Contours of constant charge densities in the $(0\bar{1}1)$ plane of zinc-blende PtN. Each contour has a value of 5.346 $\sqrt{2^n}$ millielectrons per bohr^3 and is labeled with the value of n (except for contours in the core region which are too close together to label).

three electrons of the continuum below E_F. They consist mainly of Pt 5*d* electrons but with some Pt 6*s* and 6*p* and N 2*p* hybridized in. Although metallic they give some contribution to the covalent bonding. A contour plot of the total charge density in a $(0\bar{1}1)$ plane is displayed in Fig. 5. The minimum contour is 5.346 millielectrons/bohr^3 and the contours vary by a factor of $\sqrt{2}$. The minimum charge density in the bonding region is 107 millielectrons/bohr^3. This is about 24.4% larger than the charge density in the middle of the Si covalent bond.[12]

In conclusion, we have calculated the lattice constant and bulk modulus of PtN in exact agreement with experiment and thus confirmed that PtN is the first transition-metal zinc-blende crystal as well as being the first zinc-blende metal. We further found that the rocksalt structure had a smaller cohesive energy than the zinc–blende and that its bulk modulus and the lattice constant did not agree with experiment. However, we suggested that metastable rocksalt PtN might be synthesized and that it would have a bulk modulus close to that of diamond. And finally, we parsed the zinc-blende energy bands into four components and discussed the covalent nature of each.

This work was supported by the Welch Foundation (Houston, TX) and the Texas Advanced Computing Center (TACC), University of Texas at Austin.

[1] E. Gregoryanz, C. Sanloup, M. Somayazulu, J. Badro, G. Fiquet, H-.K. Mao, and R. Hemley, Nat. Mater. **3**, 294 (2004).

[2] B. R. Sahu and Leonard Kleinman, Phys. Rev. B **68**, 113101 (2003).

[3] K. Suzuki, Y. Yamaguchi, T. Kaneko, H. Yoshida, Y. Obi, H. Fujimori, and H. Morita, J. Phys. Soc. Jpn. **70**(4), 1084 (2001).

[4] E. V. Yakovenko, I. V. Aleksandrov, A. F. Goncharov, and S. M. Stishov, Sov. Phys. JETP **68**, 1213 (1989).

[5] P. Blaha, K. Schwarz, G. K. H. Madsen, D. Kvasnicka, and J. Luitz, WIEN2K (Vienna University of Technology, Vienna, Austria, 2001).

[6] J. P. Perdew, K. Burke, and M. Ernzerhof, Phys. Rev. Lett. **77**, 3865 (1996).

[7] E. Sjöstedt, L. Nordström, and D. J. Singh, Solid State Commun. **114**, 15 (2000).

[8] G. K. H. Madsen, P. Blaha, K. Schwarz, E. Sjöstedt, and L. Nordström, Phys. Rev. B **64**, 195134 (2001).

[9] F. D. Murnaghan, Proc. Natl. Acad. Sci. U.S.A. **30**, 244 (1944).

[10] Staroverov *et al.* (Ref. 11) compared the calculated GGA lattice constants of 18 elements and compounds with experiment. Only for Li and Na were the calculated values less than the experimental.

[11] V. N. Staroverov, G. E. Scuseria, J. Tao, and J. P. Perdew, Phys. Rev. B **69**, 075102 (2004).

[12] Z. W. Lu and A. Zunger, Acta Crystallogr., Sect. A: Found. Crystallogr. **48**, 545 (1992).